Study of Y(3S,2S)→ηY(1S) and Y(3S,2S)→π^{+}π^{-}Y(1S) hadronic transitions

J. P. Lees *et al.* (The BABAR Collaboration)

Study of $\Upsilon(3S, 2S) \to \eta\Upsilon(1S)$ and $\Upsilon(3S, 2S) \to \pi^+\pi^-\Upsilon(1S)$ hadronic transitions

J. P. Lees,[1] V. Poireau,[1] V. Tisserand,[1] J. Garra Tico,[2] E. Grauges,[2] M. Martinelli[ab],[3] D. A. Milanes[a],[3]
A. Palano[ab],[3] M. Pappagallo[ab],[3] G. Eigen,[4] B. Stugu,[4] D. N. Brown,[5] L. T. Kerth,[5] Yu. G. Kolomensky,[5]
G. Lynch,[5] H. Koch,[6] T. Schroeder,[6] D. J. Asgeirsson,[7] C. Hearty,[7] T. S. Mattison,[7] J. A. McKenna,[7] A. Khan,[8]
V. E. Blinov,[9] A. R. Buzykaev,[9] V. P. Druzhinin,[9] V. B. Golubev,[9] E. A. Kravchenko,[9] A. P. Onuchin,[9]
S. I. Serednyakov,[9] Yu. I. Skovpen,[9] E. P. Solodov,[9] K. Yu. Todyshev,[9] A. N. Yushkov,[9] M. Bondioli,[10]
D. Kirkby,[10] A. J. Lankford,[10] M. Mandelkern,[10] D. P. Stoker,[10] H. Atmacan,[11] J. W. Gary,[11] F. Liu,[11] O. Long,[11]
G. M. Vitug,[11] C. Campagnari,[12] T. M. Hong,[12] D. Kovalskyi,[12] J. D. Richman,[12] C. A. West,[12] A. M. Eisner,[13]
J. Kroseberg,[13] W. S. Lockman,[13] A. J. Martinez,[13] T. Schalk,[13] B. A. Schumm,[13] A. Seiden,[13] C. H. Cheng,[14]
D. A. Doll,[14] B. Echenard,[14] K. T. Flood,[14] D. G. Hitlin,[14] P. Ongmongkolkul,[14] F. C. Porter,[14] A. Y. Rakitin,[14]
R. Andreassen,[15] M. S. Dubrovin,[15] Z. Huard,[15] B. T. Meadows,[15] M. D. Sokoloff,[15] L. Sun,[15] P. C. Bloom,[16]
W. T. Ford,[16] A. Gaz,[16] M. Nagel,[16] U. Nauenberg,[16] J. G. Smith,[16] S. R. Wagner,[16] R. Ayad,[17, *] W. H. Toki,[17]
B. Spaan,[18] M. J. Kobel,[19] K. R. Schubert,[19] R. Schwierz,[19] D. Bernard,[20] M. Verderi,[20] P. J. Clark,[21] S. Playfer,[21]
D. Bettoni[a],[22] C. Bozzi[a],[22] R. Calabrese[ab],[22] G. Cibinetto[ab],[22] E. Fioravanti[ab],[22] I. Garzia[ab],[22] E. Luppi[ab],[22]
M. Munerato[ab],[22] M. Negrini[ab],[22] L. Piemontese[a],[22] V. Santoro,[22] R. Baldini-Ferroli,[23] A. Calcaterra,[23]
R. de Sangro,[23] G. Finocchiaro,[23] M. Nicolaci,[23] P. Patteri,[23] I. M. Peruzzi,[23, †] M. Piccolo,[23] M. Rama,[23]
A. Zallo,[23] R. Contri[ab],[24] E. Guido[ab],[24] M. Lo Vetere[ab],[24] M. R. Monge[ab],[24] S. Passaggio[a],[24] C. Patrignani[ab],[24]
E. Robutti[a],[24] B. Bhuyan,[25] V. Prasad,[25] C. L. Lee,[26] M. Morii,[26] A. J. Edwards,[27] A. Adametz,[28] J. Marks,[28]
U. Uwer,[28] F. U. Bernlochner,[29] M. Ebert,[29] H. M. Lacker,[29] T. Lueck,[29] P. D. Dauncey,[30] M. Tibbetts,[30]
P. K. Behera,[31] U. Mallik,[31] C. Chen,[32] J. Cochran,[32] W. T. Meyer,[32] S. Prell,[32] E. I. Rosenberg,[32] A. E. Rubin,[32]
A. V. Gritsan,[33] Z. J. Guo,[33] N. Arnaud,[34] M. Davier,[34] G. Grosdidier,[34] F. Le Diberder,[34] A. M. Lutz,[34]
B. Malaescu,[34] P. Roudeau,[34] M. H. Schune,[34] A. Stocchi,[34] G. Wormser,[34] D. J. Lange,[35] D. M. Wright,[35]
I. Bingham,[36] C. A. Chavez,[36] J. P. Coleman,[36] J. R. Fry,[36] E. Gabathuler,[36] D. E. Hutchcroft,[36] D. J. Payne,[36]
C. Touramanis,[36] A. J. Bevan,[37] F. Di Lodovico,[37] R. Sacco,[37] M. Sigamani,[37] G. Cowan,[38] D. N. Brown,[39]
C. L. Davis,[39] A. G. Denig,[40] M. Fritsch,[40] W. Gradl,[40] A. Hafner,[40] E. Prencipe,[40] K. E. Alwyn,[41] D. Bailey,[41]
R. J. Barlow,[41, ‡] G. Jackson,[41] G. D. Lafferty,[41] E. Behn,[42] R. Cenci,[42] B. Hamilton,[42] A. Jawahery,[42]
D. A. Roberts,[42] G. Simi,[42] C. Dallapiccola,[43] R. Cowan,[44] D. Dujmic,[44] G. Sciolla,[44] D. Lindemann,[45]
P. M. Patel,[45] S. H. Robertson,[45] M. Schram,[45] P. Biassoni[ab],[46] A. Lazzaro[ab],[46] V. Lombardo[a],[46] N. Neri[ab],[46]
F. Palombo[ab],[46] S. Stracka[ab],[46] L. Cremaldi,[47] R. Godang,[47, §] R. Kroeger,[47] P. Sonnek,[47] D. J. Summers,[47]
X. Nguyen,[48] P. Taras,[48] G. De Nardo[ab],[49] D. Monorchio[ab],[49] G. Onorato[ab],[49] C. Sciacca[ab],[49] G. Raven,[50]
H. L. Snoek,[50] C. P. Jessop,[51] K. J. Knoepfel,[51] J. M. LoSecco,[51] W. F. Wang,[51] K. Honscheid,[52] R. Kass,[52]
J. Brau,[53] R. Frey,[53] N. B. Sinev,[53] D. Strom,[53] E. Torrence,[53] E. Feltresi[ab],[54] N. Gagliardi[ab],[54] M. Margoni[ab],[54]
M. Morandin[a],[54] M. Posocco[a],[54] M. Rotondo[a],[54] F. Simonetto[ab],[54] R. Stroili[ab],[54] S. Akar,[55] E. Ben-Haim,[55]
M. Bomben,[55] G. R. Bonneaud,[55] H. Briand,[55] G. Calderini,[55] J. Chauveau,[55] O. Hamon,[55] Ph. Leruste,[55]
G. Marchiori,[55] J. Ocariz,[55] S. Sitt,[55] M. Biasini[ab],[56] E. Manoni[ab],[56] S. Pacetti[ab],[56] A. Rossi[ab],[56] C. Angelini[ab],[57]
G. Batignani[ab],[57] S. Bettarini[ab],[57] M. Carpinelli[ab],[57, ¶] G. Casarosa[ab],[57] A. Cervelli[ab],[57] F. Forti[ab],[57]
M. A. Giorgi[ab],[57] A. Lusiani[ac],[57] B. Oberhof[ab],[57] E. Paoloni[ab],[57] A. Perez[a],[57] G. Rizzo[ab],[57] J. J. Walsh[a],[57]
D. Lopes Pegna,[58] C. Lu,[58] J. Olsen,[58] A. J. S. Smith,[58] A. V. Telnov,[58] F. Anulli[a],[59] G. Cavoto[a],[59] R. Faccini[ab],[59]
F. Ferrarotto[a],[59] F. Ferroni[ab],[59] M. Gaspero[ab],[59] L. Li Gioi[a],[59] M. A. Mazzoni[a],[59] G. Piredda[a],[59] C. Bünger,[60]
O. Grünberg,[60] T. Hartmann,[60] T. Leddig,[60] H. Schröder,[60] R. Waldi,[60] T. Adye,[61] E. O. Olaiya,[61] F. F. Wilson,[61]
S. Emery,[62] G. Hamel de Monchenault,[62] G. Vasseur,[62] Ch. Yèche,[62] D. Aston,[63] D. J. Bard,[63] R. Bartoldus,[63]
C. Cartaro,[63] M. R. Convery,[63] J. Dorfan,[63] G. P. Dubois-Felsmann,[63] W. Dunwoodie,[63] R. C. Field,[63] M. Franco
Sevilla,[63] B. G. Fulsom,[63] A. M. Gabareen,[63] M. T. Graham,[63] P. Grenier,[63] C. Hast,[63] W. R. Innes,[63]
M. H. Kelsey,[63] H. Kim,[63] P. Kim,[63] M. L. Kocian,[63] D. W. G. S. Leith,[63] P. Lewis,[63] S. Li,[63] B. Lindquist,[63]
S. Luitz,[63] V. Luth,[63] H. L. Lynch,[63] D. B. MacFarlane,[63] D. R. Muller,[63] H. Neal,[63] S. Nelson,[63] I. Ofte,[63]
M. Perl,[63] T. Pulliam,[63] B. N. Ratcliff,[63] A. Roodman,[63] A. A. Salnikov,[63] R. H. Schindler,[63] A. Snyder,[63] D. Su,[63]
M. K. Sullivan,[63] J. Va'vra,[63] A. P. Wagner,[63] M. Weaver,[63] W. J. Wisniewski,[63] M. Wittgen,[63] D. H. Wright,[63]
H. W. Wulsin,[63] A. K. Yarritu,[63] C. C. Young,[63] V. Ziegler,[63] W. Park,[64] M. V. Purohit,[64] R. M. White,[64]
J. R. Wilson,[64] A. Randle-Conde,[65] S. J. Sekula,[65] M. Bellis,[66] J. F. Benitez,[66] P. R. Burchat,[66] T. S. Miyashita,[66]

M. S. Alam,[67] J. A. Ernst,[67] R. Gorodeisky,[68] N. Guttman,[68] D. R. Peimer,[68] A. Soffer,[68] P. Lund,[69]
S. M. Spanier,[69] R. Eckmann,[70] J. L. Ritchie,[70] A. M. Ruland,[70] C. J. Schilling,[70] R. F. Schwitters,[70] B. C. Wray,[70]
J. M. Izen,[71] X. C. Lou,[71] F. Bianchi[ab],[72] D. Gamba[ab],[72] L. Lanceri[ab],[73] L. Vitale[ab],[73] F. Martinez-Vidal,[74]
A. Oyanguren,[74] H. Ahmed,[75] J. Albert,[75] Sw. Banerjee,[75] H. H. F. Choi,[75] G. J. King,[75] R. Kowalewski,[75]
M. J. Lewczuk,[75] I. M. Nugent,[75] J. M. Roney,[75] R. J. Sobie,[75] N. Tasneem,[75] T. J. Gershon,[76] P. F. Harrison,[76]
T. E. Latham,[76] E. M. T. Puccio,[76] H. R. Band,[77] S. Dasu,[77] Y. Pan,[77] R. Prepost,[77] and S. L. Wu[77]

(The BABAR Collaboration)

[1]*Laboratoire d'Annecy-le-Vieux de Physique des Particules (LAPP),
Université de Savoie, CNRS/IN2P3, F-74941 Annecy-Le-Vieux, France*
[2]*Universitat de Barcelona, Facultat de Fisica, Departament ECM, E-08028 Barcelona, Spain*
[3]*INFN Sezione di Bari[a]; Dipartimento di Fisica, Università di Bari[b], I-70126 Bari, Italy*
[4]*University of Bergen, Institute of Physics, N-5007 Bergen, Norway*
[5]*Lawrence Berkeley National Laboratory and University of California, Berkeley, California 94720, USA*
[6]*Ruhr Universität Bochum, Institut für Experimentalphysik 1, D-44780 Bochum, Germany*
[7]*University of British Columbia, Vancouver, British Columbia, Canada V6T 1Z1*
[8]*Brunel University, Uxbridge, Middlesex UB8 3PH, United Kingdom*
[9]*Budker Institute of Nuclear Physics, Novosibirsk 630090, Russia*
[10]*University of California at Irvine, Irvine, California 92697, USA*
[11]*University of California at Riverside, Riverside, California 92521, USA*
[12]*University of California at Santa Barbara, Santa Barbara, California 93106, USA*
[13]*University of California at Santa Cruz, Institute for Particle Physics, Santa Cruz, California 95064, USA*
[14]*California Institute of Technology, Pasadena, California 91125, USA*
[15]*University of Cincinnati, Cincinnati, Ohio 45221, USA*
[16]*University of Colorado, Boulder, Colorado 80309, USA*
[17]*Colorado State University, Fort Collins, Colorado 80523, USA*
[18]*Technische Universität Dortmund, Fakultät Physik, D-44221 Dortmund, Germany*
[19]*Technische Universität Dresden, Institut für Kern- und Teilchenphysik, D-01062 Dresden, Germany*
[20]*Laboratoire Leprince-Ringuet, Ecole Polytechnique, CNRS/IN2P3, F-91128 Palaiseau, France*
[21]*University of Edinburgh, Edinburgh EH9 3JZ, United Kingdom*
[22]*INFN Sezione di Ferrara[a]; Dipartimento di Fisica, Università di Ferrara[b], I-44100 Ferrara, Italy*
[23]*INFN Laboratori Nazionali di Frascati, I-00044 Frascati, Italy*
[24]*INFN Sezione di Genova[a]; Dipartimento di Fisica, Università di Genova[b], I-16146 Genova, Italy*
[25]*Indian Institute of Technology Guwahati, Guwahati, Assam, 781 039, India*
[26]*Harvard University, Cambridge, Massachusetts 02138, USA*
[27]*Harvey Mudd College, Claremont, California 91711*
[28]*Universität Heidelberg, Physikalisches Institut, Philosophenweg 12, D-69120 Heidelberg, Germany*
[29]*Humboldt-Universität zu Berlin, Institut für Physik, Newtonstr. 15, D-12489 Berlin, Germany*
[30]*Imperial College London, London, SW7 2AZ, United Kingdom*
[31]*University of Iowa, Iowa City, Iowa 52242, USA*
[32]*Iowa State University, Ames, Iowa 50011-3160, USA*
[33]*Johns Hopkins University, Baltimore, Maryland 21218, USA*
[34]*Laboratoire de l'Accélérateur Linéaire, IN2P3/CNRS et Université Paris-Sud 11,
Centre Scientifique d'Orsay, B. P. 34, F-91898 Orsay Cedex, France*
[35]*Lawrence Livermore National Laboratory, Livermore, California 94550, USA*
[36]*University of Liverpool, Liverpool L69 7ZE, United Kingdom*
[37]*Queen Mary, University of London, London, E1 4NS, United Kingdom*
[38]*University of London, Royal Holloway and Bedford New College, Egham, Surrey TW20 0EX, United Kingdom*
[39]*University of Louisville, Louisville, Kentucky 40292, USA*
[40]*Johannes Gutenberg-Universität Mainz, Institut für Kernphysik, D-55099 Mainz, Germany*
[41]*University of Manchester, Manchester M13 9PL, United Kingdom*
[42]*University of Maryland, College Park, Maryland 20742, USA*
[43]*University of Massachusetts, Amherst, Massachusetts 01003, USA*
[44]*Massachusetts Institute of Technology, Laboratory for Nuclear Science, Cambridge, Massachusetts 02139, USA*
[45]*McGill University, Montréal, Québec, Canada H3A 2T8*
[46]*INFN Sezione di Milano[a]; Dipartimento di Fisica, Università di Milano[b], I-20133 Milano, Italy*
[47]*University of Mississippi, University, Mississippi 38677, USA*
[48]*Université de Montréal, Physique des Particules, Montréal, Québec, Canada H3C 3J7*
[49]*INFN Sezione di Napoli[a]; Dipartimento di Scienze Fisiche,
Università di Napoli Federico II[b], I-80126 Napoli, Italy*
[50]*NIKHEF, National Institute for Nuclear Physics and High Energy Physics, NL-1009 DB Amsterdam, The Netherlands*
[51]*University of Notre Dame, Notre Dame, Indiana 46556, USA*
[52]*Ohio State University, Columbus, Ohio 43210, USA*

^{53}*University of Oregon, Eugene, Oregon 97403, USA*
^{54}*INFN Sezione di Padova^a; Dipartimento di Fisica, Università di Padova^b, I-35131 Padova, Italy*
^{55}*Laboratoire de Physique Nucléaire et de Hautes Energies,*
IN2P3/CNRS, Université Pierre et Marie Curie-Paris6,
Université Denis Diderot-Paris7, F-75252 Paris, France
^{56}*INFN Sezione di Perugia^a; Dipartimento di Fisica, Università di Perugia^b, I-06100 Perugia, Italy*
^{57}*INFN Sezione di Pisa^a; Dipartimento di Fisica,*
Università di Pisa^b; Scuola Normale Superiore di Pisa^c, I-56127 Pisa, Italy
^{58}*Princeton University, Princeton, New Jersey 08544, USA*
^{59}*INFN Sezione di Roma^a; Dipartimento di Fisica,*
Università di Roma La Sapienza^b, I-00185 Roma, Italy
^{60}*Universität Rostock, D-18051 Rostock, Germany*
^{61}*Rutherford Appleton Laboratory, Chilton, Didcot, Oxon, OX11 0QX, United Kingdom*
^{62}*CEA, Irfu, SPP, Centre de Saclay, F-91191 Gif-sur-Yvette, France*
^{63}*SLAC National Accelerator Laboratory, Stanford, California 94309 USA*
^{64}*University of South Carolina, Columbia, South Carolina 29208, USA*
^{65}*Southern Methodist University, Dallas, Texas 75275, USA*
^{66}*Stanford University, Stanford, California 94305-4060, USA*
^{67}*State University of New York, Albany, New York 12222, USA*
^{68}*Tel Aviv University, School of Physics and Astronomy, Tel Aviv, 69978, Israel*
^{69}*University of Tennessee, Knoxville, Tennessee 37996, USA*
^{70}*University of Texas at Austin, Austin, Texas 78712, USA*
^{71}*University of Texas at Dallas, Richardson, Texas 75083, USA*
^{72}*INFN Sezione di Torino^a; Dipartimento di Fisica Sperimentale, Università di Torino^b, I-10125 Torino, Italy*
^{73}*INFN Sezione di Trieste^a; Dipartimento di Fisica, Università di Trieste^b, I-34127 Trieste, Italy*
^{74}*IFIC, Universitat de Valencia-CSIC, E-46071 Valencia, Spain*
^{75}*University of Victoria, Victoria, British Columbia, Canada V8W 3P6*
^{76}*Department of Physics, University of Warwick, Coventry CV4 7AL, United Kingdom*
^{77}*University of Wisconsin, Madison, Wisconsin 53706, USA*

We study the $\Upsilon(3S, 2S) \to \eta\Upsilon(1S)$ and $\Upsilon(3S, 2S) \to \pi^+\pi^-\Upsilon(1S)$ transitions with 122×10^6 $\Upsilon(3S)$ and 100×10^6 $\Upsilon(2S)$ mesons collected by the *BABAR* detector at the PEP-II asymmetric-energy e^+e^- collider. We measure $\mathcal{B}[\Upsilon(2S) \to \eta\Upsilon(1S)] = (2.39 \pm 0.31(\text{stat.}) \pm 0.14(\text{syst.})) \times 10^{-4}$ and $\Gamma[\Upsilon(2S) \to \eta\Upsilon(1S)]/\Gamma[\Upsilon(2S) \to \pi^+\pi^-\Upsilon(1S)] = (1.35 \pm 0.17(\text{stat.}) \pm 0.08(\text{syst.})) \times 10^{-3}$. We find no evidence for $\Upsilon(3S) \to \eta\Upsilon(1S)$ and obtain $\mathcal{B}[\Upsilon(3S) \to \eta\Upsilon(1S)] < 1.0 \times 10^{-4}$ and $\Gamma[\Upsilon(3S) \to \eta\Upsilon(1S)]/\Gamma[\Upsilon(3S) \to \pi^+\pi^-\Upsilon(1S)] < 2.3 \times 10^{-3}$ as upper limits at the 90% confidence level. We also provide improved measurements of the $\Upsilon(2S)-\Upsilon(1S)$ and $\Upsilon(3S)-\Upsilon(1S)$ mass differences, $562.170 \pm 0.007(\text{stat.}) \pm 0.088(\text{syst.})$ MeV/c^2 and $893.813 \pm 0.015(\text{stat.}) \pm 0.107(\text{syst.})$ MeV/c^2, respectively.

PACS numbers: 14.40.Pq,13.25.Gv

The QCD multipole expansion (QCDME) model [1] describes hadronic transitions between heavy quarkonia. Despite its success for hadronic transitions in charmonium, this model has limits in explaining all hadronic transitions in the bottomonium spectrum. The QCDME predicts the suppression of the transitions between bottomonia via a η meson with respect to those via a dipion, the former being associated with the spin-flip effects of the b quark. The $\Upsilon(4S) \to \eta\Upsilon(1S)$ and $\Upsilon(2S) \to \eta\Upsilon(1S)$ transitions have been observed at rates significantly dif-

ferent from the predicted values [2, 3]. The measured width $\Gamma[\Upsilon(2S) \to \eta\Upsilon(1S)]$ is smaller than predicted, while $\Gamma[\Upsilon(4S) \to \eta\Upsilon(1S)]$ is larger than $\Gamma[\Upsilon(4S) \to \pi^+\pi^-\Upsilon(1S)]$, although it was expected to be suppressed in analogy with decays of the lower-mass Υ resonances. Some suggest that the latter result could be related to above-$B\overline{B}$ threshold effects [4, 5]. The $\Upsilon(3S) \to \eta\Upsilon(1S)$ transitions have not been observed [2]. Precise measurements of the transitions between bottomonia via a η meson, as well as their rate with respect to the dipion transitions could shed light on the chromomagnetic moment of the b quark.

In this paper we study the transitions $\Upsilon(nS) \to \eta\Upsilon(1S)$ and $\Upsilon(nS) \to \pi^+\pi^-\Upsilon(1S)$ with $n = 3, 2$ and measure the ratios of partial widths $\Gamma[\Upsilon(nS) \to \eta\Upsilon(1S)]/\Gamma[\Upsilon(nS) \to \pi^+\pi^-\Upsilon(1S)]$. The transitions are studied for events in which the $\Upsilon(1S)$ decays to either $\mu^+\mu^-$ or e^+e^-. The η meson is reconstructed from its $\gamma\gamma$ and $\pi^+\pi^-\pi^0$ decay modes, where the π^0 decays to $\gamma\gamma$. The analysis thus considers the final states $\pi^+\pi^-\gamma\gamma\ell^+\ell^-$,

$\gamma\gamma\ell^+\ell^-$ and $\pi^+\pi^-\ell^+\ell^-$, where $\ell = e$ or μ.

We analyze *BABAR* data samples consisting of $(121.8 \pm 1.2) \times 10^6$ $\Upsilon(3S)$ and $(98.6 \pm 0.9) \times 10^6$ $\Upsilon(2S)$ mesons. These correspond to integrated luminosities of 28.0 fb^{-1} and 13.6 fb^{-1}, respectively. We use 2.6 fb^{-1} collected 30 MeV below the $\Upsilon(3S)$ resonance, and 1.4 fb^{-1} collected 30 MeV below the $\Upsilon(2S)$ resonance ("off-peak" samples) for background studies.

The *BABAR* detector is described in detail elsewhere [6, 7]. We briefly mention the features relevant to this analysis. Charged-particle momenta are measured in a five-layer double-sided silicon vertex tracker (SVT) and a 40-layer central drift chamber (DCH), both embedded in a 1.5-T axial magnetic field. Charged-particle identification is based on specific energy loss in the SVT and the DCH and on measurements of the photons produced in the fused-silica bars of a ring-imaging Cherenkov detector. A CsI(Tl) electromagnetic calorimeter (EMC) is used to detect and identify photons and to identify electrons, while muons are identified in the instrumented flux return of the magnet (IFR).

Monte Carlo (MC) simulated events, used for efficiency determination and selection optimization, are generated with `EvtGen` [8]; `GEANT` 4 [9] is used to simulate the detector response. The variations of conditions and beam backgrounds are taken into account in the simulation. The simulated events are then analyzed in the same manner as data. Large MC samples simulating inclusive $\Upsilon(3S)$ and $\Upsilon(2S)$ decays including all known and predicted transitions and continuum $e^+e^- \to e^+e^-(\gamma)$ and $e^+e^- \to \mu^+\mu^-(\gamma)$ processes are used to characterize the backgrounds. Background from continuum quark production is negligible. In the MC signal samples, the distribution of generated dilepton decays incorporates the $\Upsilon(1S)$ polarization. Dipion transitions are modeled according to the matrix elements measured by CLEO [10]. The angular distribution in $\Upsilon(3S,2S) \to \eta\Upsilon(1S)$ processes is generated as a vector decaying to a pseudoscalar and a vector. The $\eta \to \pi^+\pi^-\pi^0$ decays are modeled according to the known Dalitz plot parameters [11]. Final state radiation effects are described by `PHOTOS` [12].

Events of interest contain two oppositely charged particles, identified as either electrons or muons. A fit constrains them to originate from a common vertex and to have invariant mass $M_{\ell\ell}$ equal to the known $\Upsilon(1S)$ mass [11]. The fit must yield a χ^2 probability $> 10^{-5}$. Muon identification is based on the energy deposited in the EMC, and the number of coordinates and interaction lengths traversed in the IFR. Electron identification is based on specific energy loss in the SVT and DCH combined with energy deposition in the EMC. Bremsstrahlung energy loss is partially recovered by an algorithm combining the energy of an electron candidate with the energies of nearby photons.

Besides the lepton pair, we require a pair of oppositely charged tracks not identified as electrons and/or two neutral particles identified as photon candidates. Events with additional charged tracks are rejected. A fit constrains all final state particles to originate from a common vertex, to have a total energy equal to the sum of the beam energies, and an invariant mass equal to the $\Upsilon(3S)$ or $\Upsilon(2S)$ mass [11]. The fit must yield a χ^2 probability $> 10^{-5}$.

A trigger-level prescaling of Bhabha scattering events, whose signature is given by two electrons of large invariant mass and no additional charged track of transverse momentum $> 250 \,\mathrm{MeV}/c$, causes the efficiency for the final states containing electrons to be smaller than for final states with muons. The di-electron efficiency drops to ~ 0 for $\Upsilon(2S)$ transitions in all final states considered, and it is $< 3\%$ for $\Upsilon(3S) \to \eta\Upsilon(1S)$ in the $\gamma\gamma e^+e^-$ final state. These final states are not considered further.

The event selection criteria have been optimized separately for each final state. The background contributions have been studied using MC samples of inclusive $\Upsilon(nS)$ decays and of $e^+e^-(\gamma)$ and $\mu^+\mu^-(\gamma)$ events. The MC background yield has been compared to real background yield from data and found to be compatible with it within the uncertainties. Also it has been verified that the distributions of all the discriminating variables are well-described by the MC background.

No further selection is applied for the $\pi^+\pi^-\ell^+\ell^-$ final states, while the additional requirements summarized in Table I are needed for the other final states. To select the $\pi^+\pi^-\gamma\gamma\ell^+\ell^-$ final states we require that the two-photon invariant mass $M_{\gamma\gamma}$ be compatible with the π^0 mass. Background events are rejected by applying selection criteria to the opening angle between the two pions, calculated in the e^+e^- center-of-mass (CM) frame ($\theta^*_{\pi\pi}$), and also to the invariant mass of the dipion candidate calculated assuming the electron mass hypothesis (M_{conv}). In particular for the $\pi^+\pi^-\gamma\gamma e^+e^-$ states, $M_{conv} > 30$ MeV suppresses events in which a photon converts in the detector material and the electrons are reconstructed as pions. In the $\Upsilon(3S) \to \eta\Upsilon(1S)$ final state, cross-feed from $\Upsilon(3S,2S) \to \pi^+\pi^-\Upsilon(2S,1S)$ transitions is suppressed by vetoing events with $\Delta M_{\pi\pi} \equiv M_{\pi\pi\ell\ell} - M_{\ell\ell}$ compatible with any of the known mass differences between narrow Υ resonances. In the $\gamma\gamma\mu^+\mu^-$ final states, the backgrounds due to the radiative transitions $\Upsilon(nS) \to \gamma\chi_{bJ}(2P,1P)$ with $\chi_{bJ}(2P,1P) \to \gamma\Upsilon(1S)$ are rejected by vetoing events where either photon energy calculated in the CM frame ($E^*_{\gamma 1,\gamma 2}$) is compatible with any of those transitions. The background from $\mu^+\mu^-(\gamma)$ events is reduced by requirements on the opening angle between the two photons ($\theta^*_{\gamma\gamma}$), and on the momentum of each lepton ($p^*_{\ell\pm}$) in the CM frame.

The signal yields are extracted with a 2-dimensional, unbinned, extended, maximum-likelihood fit to the measured distribution of a pair of variables. For the $\Upsilon(nS) \to \pi^+\pi^-\Upsilon(1S)$ transitions we fit the $\Delta M_{\pi\pi}$ versus $M_{\ell\ell}$ distribution, both calculated from the measured values prior to the invariant mass constraint (Fig. 1). For the $\Upsilon(nS) \to \eta\Upsilon(1S)$ transitions with $\eta \to \pi^+\pi^-\pi^0$ decays, we fit the ΔM_η versus $M_{\pi\pi\gamma\gamma}$ distribution, where $\Delta M_\eta \equiv M_{\pi\pi\gamma\gamma\ell\ell} - M_{\ell\ell} - M_{\pi\pi\gamma\gamma}$ and $M_{\pi\pi\gamma\gamma}$ is the in-

TABLE I: Additional requirements applied to select $\pi^+\pi^-\gamma\gamma\ell^+\ell^-$ and $\gamma\gamma\ell^+\ell^-$ final states. Masses are expressed in MeV/c^2, energies in GeV, and momenta in GeV/c.

$\Upsilon(2S) \to \eta\Upsilon(1S)$	$\Upsilon(3S) \to \eta\Upsilon(1S)$	
$\pi^+\pi^-\gamma\gamma\mu^+\mu^-$	$\pi^+\pi^-\gamma\gamma\mu^+\mu^-$	$\pi^+\pi^-\gamma\gamma e^+e^-$
$M_{conv} < 310$	$M_{conv} < 280$	$30 < M_{conv} < 280$
$90 < M_{\gamma\gamma} < 180$	$100 < M_{\gamma\gamma} < 170$	$90 < M_{\gamma\gamma} < 150$
$\cos\theta^*_{\pi\pi} < 0$		
	$(400 < \Delta M_{\pi\pi} < 550) \cup (\Delta M_{\pi\pi} > 580)$	
$\gamma\gamma\mu^+\mu^-$	$\gamma\gamma\mu^+\mu^-$	
$200 < E^*_{\gamma1,\gamma2} < 350$	$(120 < E^*_{\gamma1} < 360) \cup (490 < E^*_{\gamma1} < 660)$	
	$(130 < E^*_{\gamma2} < 370) \cup (470 < E^*_{\gamma2} < 700)$	
$\cos\theta^*_{\gamma\gamma} < -0.86$	$-0.45 < \cos\theta^*_{\gamma\gamma} < 0.22$	
$4.60 < p^*_{\ell\pm} < 4.85$	$4.4 < p^*_{\ell+} < 5.0$; $4.4 < p^*_{\ell-} < 5.1$	

variant mass of the η decay products (Fig. 2). For the $\Upsilon(nS) \to \eta\Upsilon(1S)$ transitions with $\eta \to \gamma\gamma$ decays, we fit the $\Delta M'_\eta$ versus $M_{\gamma\gamma}$ distribution, where $\Delta M'_\eta \equiv M_{\gamma\gamma\ell\ell} - M_{\ell\ell} - M_{\gamma\gamma}$ (Fig. 3).

Each observed distribution is fit to a sum of a signal and a background component. The functional form of the probability density functions (PDFs) for signal and background have been determined from MC samples. The signal PDFs are described by double or triple Gaussian functions, or by a Gaussian-like analytical function with mean value μ but different widths, $\sigma_{L,R}$, on the left side (for $x < \mu$) and on the right side (for $x > \mu$) plus asymmetric tails $\alpha_{L,R}$, defined as:

$$\mathcal{F}(x) = \exp\left\{ -\frac{(x-\mu)^2}{2\sigma^2_{L,R} + \alpha_{L,R}(x-\mu)^2} \right\}. \qquad (1)$$

The PDFs used to model the signal and background shapes in each fit are given in Table II. The free parameters in each fit are the signal and background yields and the parameter of the background PDFs of Table II. The signal shape parameters are also floated in the fits to the $\Upsilon(nS) \to \pi^+\pi^-\ell^+\ell^-$ samples, while they are fixed to the values determined from MC samples in all other cases.

The number of signal candidates returned by the fits is reported in Table III. We estimate the signal significance in standard deviations as $\sqrt{2\log[\mathcal{L}(N)/\mathcal{L}(0)]}$, where $\mathcal{L}(N)/\mathcal{L}(0)$ is the ratio between the likelihood values for a fit that includes a signal yield N and a fit with a background hypothesis only. For the $\Upsilon(2S) \to \eta\Upsilon(1S)$ transition the signal significance is 8.0σ for the $\pi^+\pi^-\gamma\gamma\mu^+\mu^-$ final states and 8.5σ for the $\gamma\gamma\mu^+\mu^-$ ones. For the $\Upsilon(3S) \to \eta\Upsilon(1S)$ we find no evidence of a signal in any of the final states considered and calculate 90% CL upper limits on the number of signal events (N_{UL}) as $\int_0^{N_{UL}} \mathcal{L}(N)dN = 0.9 \times \int_0^\infty \mathcal{L}(N)dN$. The efficiencies with which signal events satisfy the selection criteria (ϵ_{sel}) are determined using simulated signal samples. Corrections are applied to account for differences between

data and MC in lepton identification and π^0 reconstruction efficiencies. The corrected values are also reported in Table III.
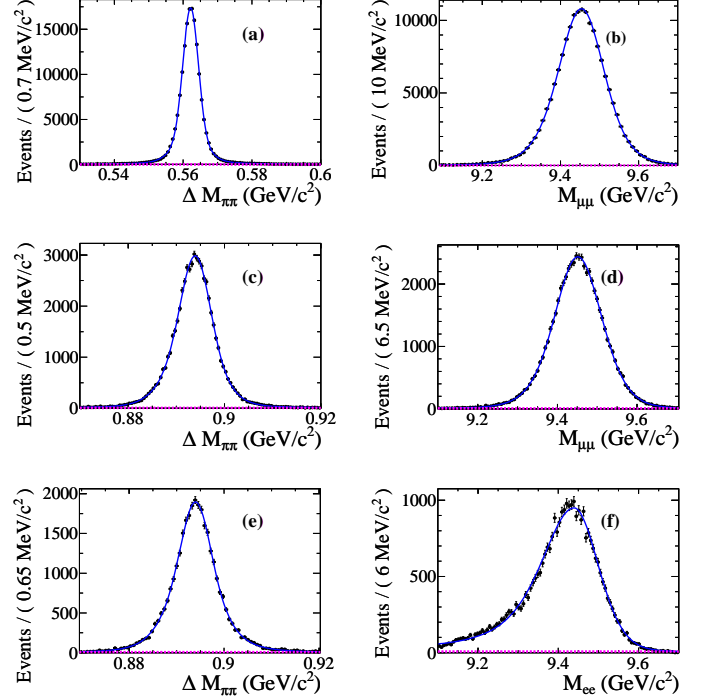

FIG. 1: $\Delta M_{\pi\pi}$ and $M_{\ell\ell}$ distributions for (a,b) $\Upsilon(2S) \to \pi^+\pi^-\Upsilon(1S) \to \pi^+\pi^-\mu^+\mu^-$ candidates, (c,d) $\Upsilon(3S) \to \pi^+\pi^-\Upsilon(1S) \to \pi^+\pi^-\mu^+\mu^-$ candidates, and (e,f) $\Upsilon(3S) \to \pi^+\pi^-\Upsilon(1S) \to \pi^+\pi^-e^+e^-$ candidates. Data are represented by dots, the fit results as solid curves and the background components by the dashed curves.
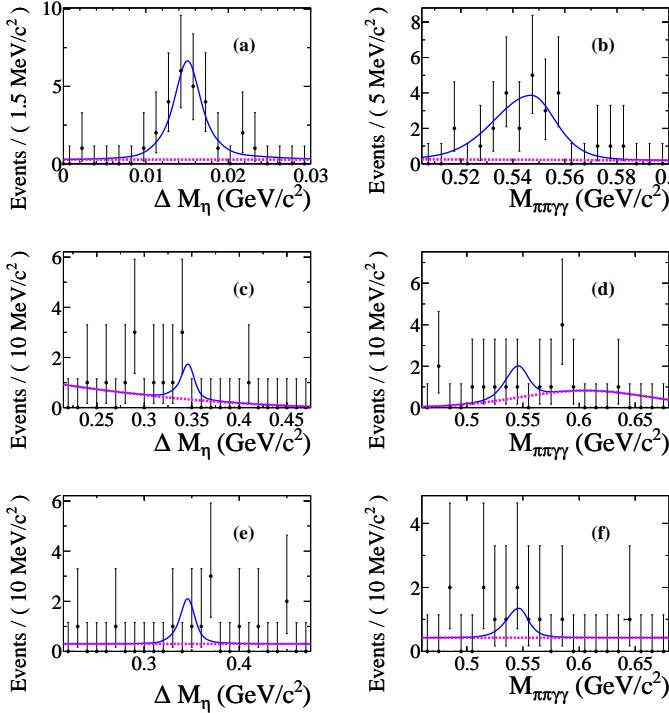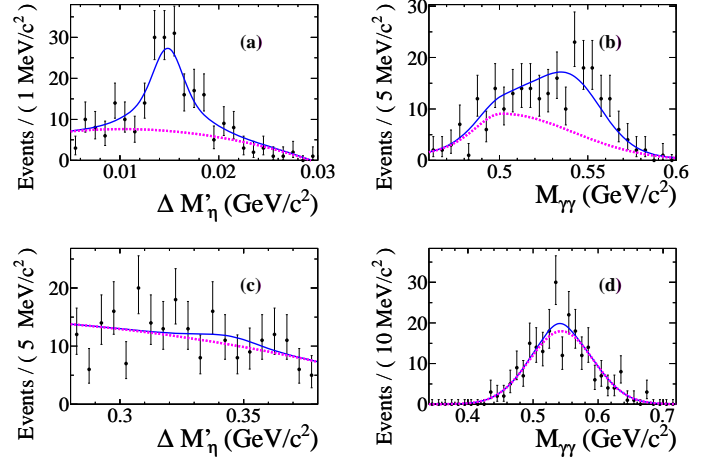
Possible sources of systematic uncertainty are considered in addition to those on the number of $\Upsilon(nS)$ (N_Υ) and on the values for secondary branching fractions ($\mathcal{B}_{secondary}$) [11]. The uncertainties on charged-particle track and single γ or π^0 reconstruction efficiencies are determined by a comparison between data and MC events using independent control samples of τ pair events, each τ decaying to either one or three charged-particle tracks. The systematic uncertainty on the muon or electron identification probability is estimated by comparing the values determined in the $\Upsilon(nS) \to \pi^+\pi^-\Upsilon(1S)$ mode in data and MC samples. For each discriminating variable, we compare the distribution for the signal component deconvolved from data with the maximum likelihood fit used for the extraction of the yields [13] to the distribution obtained in the MC. The related systematic uncertainty is estimated as the change in event selection efficiency induced by the difference between the distributions. The systematic uncertainties on the $\Delta M_{\pi\pi}$ and $E^*_{\gamma1,2}$ vetoes for cross-feed dipion and radiative transitions are estimated by comparing the corresponding efficiencies in data and MC samples. In order to take into

TABLE II: Functions used to model the signal and background PDFs.

Final state	1st Variable	Signal	Background	2nd Variable	Signal	Background
$\Upsilon(nS) \to \pi^+\pi^-\ell^+\ell^-$	$\Delta M_{\pi\pi}$	triple Gaussian	0thorder poly	$M_{\ell\ell}$	Eq.(1)	0thorder poly
$\Upsilon(2S) \to \pi^+\pi^-\gamma\gamma\mu^+\mu^-$	ΔM_η	triple Gaussian	0thorder poly	$M_{\pi\pi\gamma\gamma}$	Eq.(1)	1storder poly
$\Upsilon(2S) \to \gamma\gamma\mu^+\mu^-$	$\Delta M'_\eta$	triple Gaussian	2ndorder poly	$M_{\gamma\gamma}$	double Gaussian	Eq.(1)
$\Upsilon(3S) \to \pi^+\pi^-\gamma\gamma\ell^+\ell^-$	ΔM_η	triple Gaussian	2ndorder poly	$M_{\pi\pi\gamma\gamma}$	Eq.(1)	2ndorder poly
$\Upsilon(3S) \to \gamma\gamma\mu^+\mu^-$	$\Delta M'_\eta$	double Gaussian	1storder poly	$M_{\gamma\gamma}$	double Gaussian	Gaussian

TABLE III: Efficiencies (ϵ_{sel}) and number of signal events (N) for each channel; upper limit at 90% CL (N_{UL}) is given in parentheses. Uncertainties are statistical only.

Transition	Final state	ϵ_{sel} (%)	N
$\Upsilon(2S) \to \pi^+\pi^-\Upsilon(1S)$	$\pi^+\pi^-\mu^+\mu^-$	39.1	170061±413
$\Upsilon(2S) \to \eta\Upsilon(1S)$	$\pi^+\pi^-\gamma\gamma\mu^+\mu^-$	18.5	22±5
	$\gamma\gamma\mu^+\mu^-$	37.2	90±14
$\Upsilon(3S) \to \pi^+\pi^-\Upsilon(1S)$	$\pi^+\pi^-e^+e^-$	25.0	31330±186
	$\pi^+\pi^-\mu^+\mu^-$	42.8	58500±247
$\Upsilon(3S) \to \eta\Upsilon(1S)$	$\pi^+\pi^-\gamma\gamma e^+e^-$	18.1	4±2 (<8)
	$\pi^+\pi^-\gamma\gamma\mu^+\mu^-$	8.9	4±2 (<8)
	$\gamma\gamma\mu^+\mu^-$	18.5	7±11 (<26)

FIG. 3: $\Delta M'_\eta$ and $M_{\gamma\gamma}$ distributions for (a,b) $\Upsilon(2S) \to \eta\Upsilon(1S) \to \gamma\gamma\mu^+\mu^-$ candidates, and (c,d) $\Upsilon(3S) \to \eta\Upsilon(1S) \to \gamma\gamma\mu^+\mu^-$ candidates. Data are represented by dots, the fit results as solid curves and the background components by the dashed curves.

FIG. 2: ΔM_η and $M_{\pi\pi\gamma\gamma}$ distributions for (a,b) $\Upsilon(2S) \to \eta\Upsilon(1S) \to \pi^+\pi^-\gamma\gamma\mu^+\mu^-$ candidates, (c,d) $\Upsilon(3S) \to \eta\Upsilon(1S) \to \pi^+\pi^-\gamma\gamma\mu^+\mu^-$ candidates, and (e,f) $\Upsilon(3S) \to \eta\Upsilon(1S) \to \pi^+\pi^-\gamma\gamma e^+e^-$ candidates. Data are represented by dots, the fit results as solid curves and the background components by the dashed curves.

account possible discrepancies between simulation and data, the dipion events are generated using values for the transition matrix elements varied of ±1σ with respect to those measured by CLEO [10]. The difference in the efficiency is treated as a systematic uncertainty. The systematic uncertainty due to the choice of signal and background PDFs is estimated by using different functions, or different values for the fixed parameters. The complete list of contributions to the systematic uncertainty is summarized in Table IV. The total systematic uncertainty for each dataset is estimated by summing all the contributions in quadrature.

The value of the branching fraction ($\mathcal{B}$), or upper limit on the branching fraction, for each mode is:

$$\mathcal{B} = \frac{N}{\epsilon_{sel} \times N_\Upsilon \times \mathcal{B}_{secondary}}, \qquad (2)$$

where N is the signal yield or upper limit on the signal yield. For a given channel, when both the leptonic $\Upsilon(1S)$ decays are available, their signal yields are first combined in a weighted average, where the weight is the inverse of the squared sum of the statistical and the sys-

TABLE IV: Sources of systematic uncertainty on the branching fractions $\mathcal{B}$ and on the ratios of partial widths, for each channel analyzed. All errors are given in percent. When both of the leptonic $\Upsilon(1S)$ decays are analyzed, the values in parentheses refer to the corresponding e^+e^- final states.

Source	$\Upsilon(2S) \to$ $\pi^+\pi^-\Upsilon(1S)$	$\eta\Upsilon(1S)$ $\eta \to \pi^+\pi^-\pi^0$	$\eta \to \gamma\gamma$	$\Upsilon(3S) \to$ $\pi^+\pi^-\Upsilon(1S)$	$\eta\Upsilon(1S)$ $\eta \to \pi^+\pi^-\pi^0$	$\eta \to \gamma\gamma$
N_Υ		0.9			1.0	
Tracking	1.4	1.4	1.0	2.5	2.5	1.7
π^0/γ	-	3.6	3.6	-	3.6	3.6
Lepton identification		1.1		1.0 (1.2)	1.0 (1.2)	1.0
$\pi^+\pi^-$ model	0.5	-	-	0.4 (1.5)	-	-
Selection	0.4	2.6	5.5	0.9 (1.2)	4.4 (5.3)	5.6
PDFs	0.1	5.4	5.0	0.1	5.4	5.0
Total $\mathcal{B}$	2.9	7.6	8.7	3.6 (4.1)	8.6 (9.1)	8.1
Total ratio		7.2	8.3		8.3 (8.9)	7.8

TABLE V: Measured branching fractions and ratios of partial widths for hadronic $\Upsilon(nS)$ transitions. The first uncertainty is statistical, the second systematic. All ULs are at 90% of CL. The PDG values and the relevant predictions are given also.

		This work	PDG [11]	Predictions [1, 4, 5]
$\mathcal{B}[\Upsilon(2S) \to \eta\Upsilon(1S)]$	(10^{-4})	$2.39 \pm 0.31 \pm 0.14$	$2.1^{+0.8}_{-0.7}$	7-16
$\mathcal{B}[\Upsilon(2S) \to \pi^+\pi^-\Upsilon(1S)]$	(10^{-2})	$17.80 \pm 0.05 \pm 0.37$	18.1 ± 0.4	40
$\dfrac{\Gamma[\Upsilon(2S) \to \eta\Upsilon(1S)]}{\Gamma[\Upsilon(2S) \to \pi^+\pi^-\Upsilon(1S)]}$	(10^{-3})	$1.35 \pm 0.17 \pm 0.08$	1.2 ± 0.4	1.7-3.8
$\mathcal{B}[\Upsilon(3S) \to \eta\Upsilon(1S)]$	(10^{-4})	< 1.0	< 1.8	5-10
$\mathcal{B}[\Upsilon(3S) \to \pi^+\pi^-\Upsilon(1S)]$	(10^{-2})	$4.32 \pm 0.07 \pm 0.13$	4.40 ± 0.10	5
$\dfrac{\Gamma[\Upsilon(3S) \to \eta\Upsilon(1S)]}{\Gamma[\Upsilon(3S) \to \pi^+\pi^-\Upsilon(1S)]}$	(10^{-3})	< 2.3	< 4.2	11-20

tematic uncertainties on each yield, considering only the systematic contributions that are uncorrelated. We assume $\mathcal{B}[\Upsilon(1S) \to e^+e^-] = \mathcal{B}[\Upsilon(1S) \to \mu^+\mu^-]$ [11]. For the η transitions, the signal yields extracted from the two different η decays are combined with the same weighted average technique. The results are shown in Table V.

We can also provide improved measurements of the differences between the Υ invariant masses, using the fitted value of $\Delta M_{\pi\pi}$ for both the $\Upsilon(2S) \to \pi^+\pi^-\Upsilon(1S)$ and the $\Upsilon(3S) \to \pi^+\pi^-\Upsilon(1S)$ transitions. The values are $562.170 \pm 0.007(\text{stat.}) \pm 0.088(\text{syst.})\,\text{MeV}/c^2$ and $893.813 \pm 0.015(\text{stat.}) \pm 0.107(\text{syst.})\,\text{MeV}/c^2$, respectively, where the latter value is obtained as a weighted average of the values for the electron and muon samples. The systematic uncertainties are due mainly to the track momentum measurement, which is related to the knowledge of the amount of detector material and of the magnetic field [15].

We have presented a study of $\Upsilon(3S) \to \Upsilon(1S)$ and $\Upsilon(2S) \to \Upsilon(1S)$ hadronic transitions. We have reported an improved measurement of $\mathcal{B}[\Upsilon(2S) \to \eta\Upsilon(1S)]$ and a 90% CL UL on $\mathcal{B}[\Upsilon(3S) \to \eta\Upsilon(1S)]$ compatible with, and more precise than, earlier measurements [2], thus, further constraining theoretical predictions (see Table V). We have also presented new measurements of

$\mathcal{B}[\Upsilon(nS) \to \pi^+\pi^-\Upsilon(1S)]$ with $n = 3, 2$, which we find to be compatible with earlier measurements [11]. Using the independent BABAR measurement of $\mathcal{B}[\Upsilon(3S) \to X\Upsilon(2S)] \times \mathcal{B}[\Upsilon(2S) \to \pi^+\pi^-\Upsilon(1S)]$ in the inclusive dipion spectrum [14], we extract the value $\mathcal{B}[\Upsilon(3S) \to X\Upsilon(2S)] = (10.0 \pm 0.6)\%$.

Improved measurements of the ratios $\Gamma[\Upsilon(nS) \to \eta\Upsilon(1S)]/\Gamma[\Upsilon(nS) \to \pi^+\pi^-\Upsilon(1S)]$, for which systematic uncertainties partially cancel, have been presented also [11]. The suppression of the $\Upsilon(nS) \to \eta\Upsilon(1S)$ transitions with respect to the $\Upsilon(nS) \to \pi^+\pi^-\Upsilon(1S)$ ones is confirmed to be higher than predicted by the QCDME [1] and not compatible with other models [4, 5].

[1] Y. -P. Kuang, Front. Phys. China **1**, 19 (2006).

[2] Q. He *et al.* (CLEO Collaboration), Phys. Rev. Lett. **101**, 192001 (2008).

[3] B. Aubert *et al.* (*BABAR* Collaboration), Phys. Rev. D **78**, 112002 (2008).

[4] Yu. A. Simonov and A. I. Veselov, arXiv:0806.2919 (2008).

[5] C. Meng and K. T. Chao, Phys. Rev. D **78**, 074001 (2008).

[6] B. Aubert *et al.* (*BABAR* Collaboration), Nucl. Instrum. Meth. A **479**, 1 (2002).

[7] M. Andreotti (*BABAR* LST Collaboration), SLAC-PUB-12205 (2005).

[8] D. J. Lange, Nucl. Instrum. Meth. A **462**, 152 (2001).

[9] S. Agostinelli *et al.* (Geant4 Collaboration), Nucl. Instrum. Meth. A **506**, 250 (2003).

[10] D. Cronin-Hennessy *et al.* (CLEO Collaboration), Phys. Rev. D **76**, 072001 (2007); S. R. Bhari *et al.* (CLEO Collaboration), Phys. Rev. D **79** , 011103 (2009).

[11] K. Nakamura *et al.* (Particle Data Group), J. Phys. G **37**, 075021 (2010).

[12] E. Barberio and Z. Was, Comput. Phys. Commun. **79**, 291 (1994).

[13] M. Pivk and F. R. Le Diberder, Nucl. Instrum. Meth. A **555**, 356 (2005).

[14] J. P. Lees *et al.* (*BABAR* Collaboration), Phys. Rev. D **84**, 011104(R) (2011).

[15] B. Aubert *et al.* (*BABAR* Collaboration), Phys. Rev. D **80** , 092005 (2009).